

Constraining the nuclear symmetry energy with charge radii of the mirror pairs nuclei

Rong An,^{1,2,3} Shuai Sun,¹ Li-Gang Cao,^{1,2,*} and Feng-Shou Zhang^{1,2,4,†}

¹*Key Laboratory of Beam Technology of Ministry of Education,
College of Nuclear Science and Technology,
Beijing Normal University, Beijing 100875, China*

²*Key Laboratory of Beam Technology of Ministry of Education,
Institute of Radiation Technology, Beijing Academy
of Science and Technology, Beijing 100875, China*

³*CAS Key Laboratory of High Precision Nuclear Spectroscopy,
Institute of Modern Physics, Chinese Academy of Sciences, Lanzhou 730000, China*

⁴*Center of Theoretical Nuclear Physics,
National Laboratory of Heavy Ion Accelerator of Lanzhou, Lanzhou 730000, China*

Abstract

Nuclear charge radius provides a vital role in determining the equation of state (EoS) of isospin asymmetric nuclear matter. Based on the correlation between the differences of charge radii of mirror-partner nuclei (ΔR_{ch}) and the slope parameter (L) of symmetry energy at the nuclear saturation density, an analysis of the calibrated slope parameter L is performed in finite nuclei. In this work, the relativistic and non-relativistic energy density functionals (EDFs) are employed to make constraints on the nuclear symmetry energy through the available databases of these mirror pairs nuclei ^{36}Ca - ^{36}S , ^{38}Ca - ^{38}Ar and ^{54}Ni - ^{54}Fe . The deduced nuclear symmetry energy is firmly located at the range of 29.89-31.85 MeV and the slope parameter L of symmetry energy essentially covers the range of 22.50-51.55 MeV.

* Corresponding author: caolg@bnu.edu.cn

† Corresponding author: fszhang@bnu.edu.cn

I. INTRODUCTION

Precise knowledge of nuclear symmetry energy (NSE), which is characterized as a component of the equation of state (EoS) of isospin asymmetric nuclear matter, can provide access to various physical phenomena relevant to a broad range of density profiles and energy scales [1, 2]. The NSE plays an important role in understanding the nuclear structure. Moreover, the behavior of NSE may affect the properties of neutron stars [3–5] and help to comprehend the supernova explosion mechanism and stellar nucleosynthesis in astrophysical study [6].

The density dependence of NSE, i.e., $E_s(\rho)$, can be expanded around the saturation density ρ_0 ($\simeq 0.16 \text{ fm}^{-3}$) as follows

$$E_s(\rho) \approx E_s(\rho_0) + \frac{L}{3} \left(\frac{\rho - \rho_0}{\rho_0} \right) + \frac{K_{\text{sym}}}{18} \left(\frac{\rho - \rho_0}{\rho_0} \right)^2 + \dots, \quad (1)$$

where L and K_{sym} are the slope and curvature of symmetry energy at nuclear saturation density ρ_0 , respectively. The symmetry energy is believed to associate with the isovector sensitive indicators in the EoS of isospin asymmetric system. Unfortunately, a direct connection between the experimental observables and the EoS is not possible. As a consequence, the microscopic implications about the NSE can be extracted indirectly from the ground and collective excited state properties of atomic nuclei, reaction observables and the detected dense astrophysical events [7, 8].

So far, enormous efforts have been undertaken to determine the EoS over the spread of density profiles and energy scales [9]. The neutron skin thickness (NST) of a heavy nucleus provides an available constraint on the EoS of neutron-rich matter around ρ_0 [10–17]. In laboratory, the radius of ^{208}Pb has been detected by measuring the parity violating asymmetry in the polarised elastic electron scattering experiments, e.g., sequentially in the PREX-II [18]. The accuracy of NST has been further updated from the latest performance, namely $R_{\text{skin}}^{208} = 0.283 \pm 0.071 \text{ fm}$. The behavior of $E_s(\rho)$ is mostly governed by the slope of symmetry energy L . The correlation between R_{skin}^{208} and slope parameter L leads to the value of $L = 106 \pm 37 \text{ MeV}$ [19]. In addition, the NSE can also be investigated by using the isotopes binding energy difference [20, 21] and double magic nuclei [22, 23].

Quite noticeable progress has been made to evaluate the NSE from the collective excited state properties of finite nuclei, such as isobaric analog states [24], pygmy dipole resonance

(PDR) [25], electric dipole polarizability [26], giant dipole resonance (GDR) [27], isovector giant quadrupole resonance (IVGQR) [28] and the charge-exchange giant resonances [29–32], etc. The results for L extracted from the PDR in the ^{68}Ni and ^{132}Sn are constrained to be in the interval of 50.3-89.4 MeV and 29.0-82.0 MeV [25], respectively. The deduced slope parameter from the weighted average can cover the range of $L = 64.8 \pm 15.7$ MeV. As suggested in Ref. [28], the slope parameter of symmetry energy can be reduced to 37 ± 18 MeV by exploiting the IVGQR energies.

Moreover, the NSE offers a key requirement for our understanding of nuclear reactions under the isospin diffusions and isotopic distributions [33–35]. The heavy-ion collisions (HICs) provide a sensitive probe to link the nuclear EoS that depends on the isovector potentials. In transport models, nuclear symmetry energy is derived from simulating the isospin sensitive observables [36–40]. Hence plenty of simulation codes are desirable to determine the NSE [41–46]. More details about transport simulations can also be found in the latest study [47]. Meanwhile, new observations of compact stellar objects have provided a wealth of data that allow one to discern the EoS across saturation density [48, 49]. The range of L can be deduced from the observation of the gravitational-wave event of the neutron star merger GW170817 [50], which leads to $L = 11\text{-}65$ MeV.

The density dependence of symmetry energy is fairly uncertain except the bulk properties at saturation density ρ_0 . This challenges us to reduce the model intrinsic uncertainties from multiple aspects about the isovector components. As demonstrated in Refs. [51, 52], the difference of root-mean-square (rms) charge radii of mirror-pair nuclei (ΔR_{ch}) obtained by Skyrme functionals provides an alternative opportunity in calibrating the density dependence of NSE. A related linear correlation between ΔR_{ch} and the slope parameter L has been established. In Ref. [53], the differences of mirror-partner nuclei charge radii for ^{36}Ca - ^{36}S and ^{38}Ca - ^{38}Ar are investigated with varied values of L . It is evidently noted that the slope parameter captures the range of $L = 5\text{-}70$ MeV. The latest precise determination evaluates the correlation between the difference of charge radii of mirror-partner nuclei ^{54}Ni - ^{54}Fe and the slope parameter, which implies a range of $L = 21\text{-}88$ MeV [54]. In which the rms charge radii of nuclei ^{54}Ni and ^{54}Fe are obtained by the Skyrme energy density functionals (EDFs) and the covariant density functionals theories (CDFTs), respectively.

As demonstrated above, the ΔR_{ch} of mirror pairs nuclei can be employed to extract the information about L . The latest result of charge radii of ^{54}Ni facilitates the efficiency in

TABLE I. R_{ch} and ΔR_{ch} database for the $A = 36, 38$ and 54 mirror pairs nuclei. The parentheses on the value of charge radii and the difference of charge radii are shown with systematic uncertainties [53–55].

| A | | R_{ch} (fm) | ΔR_{ch} (fm) |
|-----|----|----------------------|-----------------------------|
| 36 | Ca | 3.4484(27) | |
| | S | 3.2982(12) | 0.150(4) |
| 38 | Ca | 3.4652(17) | |
| | Ar | 3.4022(15) | 0.063(3) |
| 54 | Ni | 3.7370(30) | |
| | Fe | 3.6880(17) | 0.049(4) |

exploring the nuclear EoS. The experimental data of R_{ch} and ΔR_{ch} for the relevant mirror partners are listed in Table I [53–55]. The NSE characterized as an isovector indicator in effective interactions should be systematically evaluated based on the latest experiment. In order to further obtain the comprehensive conclusion about the correlations between L and ΔR_{ch} , the ΔR_{ch} for the pairs of mass number $A = 36, 38$ and 54 are calculated by using the non-relativistic and relativistic (covariant) EDFs. Although the correlations between the incompressibility coefficients and the isovector parameters are generally weaker with respect to the correlations between the slope parameter L and symmetry energy [56], the uncertainty suffering from nuclear incompressibility is inevitable in evaluated process. Therefore, the values of incompressibility coefficients characterized as isoscalar parameters are almost identical for two kinds of EDFs.

This paper is organized as follows. In Sec. II, we briefly report the theoretical models. In Sec. III, we present the results and discussions. A short summary and outlook are provided in Sec. IV.

II. THEORETICAL FRAMEWORK

In this work, we adopt two kinds of widely used nuclear density functionals to extract the information about the nuclear matter EoS, namely the sophisticated Skyrme EDFs and covariant EDFs. Both of them have achieved great success in describing the structures of finite nuclei, especially global properties such as binding energies and charge radii [57–59].

In our applications, the two families parameter sets are adopted, named as the asy family for Skyrme EDFs [60] and the IUFSU family for covariant EDFs [61]. All of these effective forces were built by fitting the parameters to specific observables of finite nuclei, such as binding energies, charge radii, the isovector part of the EoS generated by such a way that the symmetry energy remains fixed value (≈ 26 MeV) at a baryon density of $\rho \approx 0.1 \text{ fm}^{-3}$, so the interactions are characterized by different values of the symmetry energy at saturation density. This procedure ensures that the quality of the fit cannot be contaminated and all isoscalar observables remain unchanged, e.g., incompressibility coefficient almost equals to 230 MeV. More details can be found in Refs. [61, 62]. It is remarkably mentioned that both symmetry energies and slope parameters can cover a wide range. In order to reduce the model intrinsic uncertainties, such parametrization sets should be expected to provide stringent constraints on the observables that are highly sensitive to the density-dependence of the symmetry energy. The corresponding values of the bulk properties of nuclear matter are shown explicitly in Table II.

TABLE II. Models used for the calculation of R_{ch} . The corresponding bulk properties of nuclear matter used in this work, such as symmetry energy E_s (MeV), the slope parameter L (MeV) and the incompressibility K_∞ (MeV) at saturation density, are given.

| Type | Sets | E_s (MeV) | L (MeV) | K_∞ (MeV) |
|--------|---------|-------------|-----------|------------------|
| RMF | IUFSU05 | 30.48 | 46.11 | 229.98 |
| | IUFSU04 | 31.52 | 52.09 | 229.98 |
| | IUFSU03 | 32.59 | 60.52 | 230.05 |
| | IUFSU02 | 33.85 | 71.83 | 230.01 |
| | IUFUS01 | 35.49 | 87.27 | 230.04 |
| | IUFSU00 | 37.16 | 108.76 | 229.88 |
| Skyrme | asy30 | 30.00 | 22.87 | 230.20 |
| | asy32 | 31.99 | 36.22 | 229.99 |
| | asy34 | 33.99 | 56.14 | 229.84 |
| | asy36 | 36.00 | 71.54 | 229.93 |
| | asy38 | 38.00 | 87.62 | 230.20 |
| | asy40 | 40.01 | 106.09 | 230.09 |

III. RESULTS AND DISCUSSIONS

The results for ΔR_{ch} are plotted as a function of L in Fig. 1. The non-relativistic Skyrme approach and the RMF theory are used to assess the correlation between ΔR_{ch} and L , which are shown by the open circles and crosses in Fig. 1, respectively. The horizontal light blue bands indicate the uncertainties of ΔR_{ch} , which correspond to 0.146-0.154 fm (^{36}Ca - ^{36}S), 0.060-0.066 fm (^{38}Ca - ^{38}Ar) and 0.045-0.053 fm (^{54}Ni - ^{54}Fe). The linear fits in the correction for ΔR_{ch} are shown using dashed lines.

Results obtained by the Skyrme EDFs and covariant EDFs display an approximate linear correlation between ΔR_{ch} and L . Constraints on L are deduced by comparing theoretical predictions with the experimental results in Fig. 1. Note that the results for $A = 54$ provides the slope of symmetry energy L relevant to the range of 17.99-62.43 MeV, for $A = 38$ and $A = 36$ are in the interval 6.83-52.49 and 22.50-51.55 MeV, respectively. One can find that these values essentially cover the theoretical uncertainties in Refs. [53, 54].

The NST of ^{48}Ca is regarded as the feasible isovector indicator to constrain the EoS of nuclear matter. The high-resolution $E1$ polarizability experiment performed in RCNP suggests that the NST of ^{48}Ca is located in the interval of 0.14 \sim 0.20 fm [63]. Meanwhile, the CREX collaboration has reported a new value through parity-violating electron scattering measurements, namely 0.071 \sim 0.171 fm [64]. The NST of ^{48}Ca will allow direct comparison to microscopic calculations with various slope parameters L . As shown in Refs. [65, 66], the linear correlation analysis of the ΔR_{ch} of mirror-partner nuclei and the corresponding NST has been clearly illustrated. Therefore, it is essential to evaluate the correlations between ΔR_{ch} of mirror pairs nuclei and the NST of ^{48}Ca .

The correlations between ΔR_{ch} of $A = 36, 38$ and 54 mirror-partner nuclei and the NST of ^{48}Ca (ΔR_{np}) are also shown in Fig. 2. The calculated ΔR_{ch} can substantially cover the current uncertainties of $\Delta R_{\text{np}}(^{48}\text{Ca})$ for both kinds of EDFs. For the $A = 54$ mirror pair nuclei, the Skyrme model gives a comparable correlation with respect to RMF model. A high linear correlation between ΔR_{ch} of $A = 54$ and ΔR_{np} of ^{48}Ca is built. For $A = 36$ and 38 mirror partners, these correlations obtained by non-relativistic and relativistic EDFs are also obviously appeared as shown in Figs. 2 (a)-(b). This means that the information content of symmetry energy can be extracted from the differences of charge radii of mirror pairs nuclei.

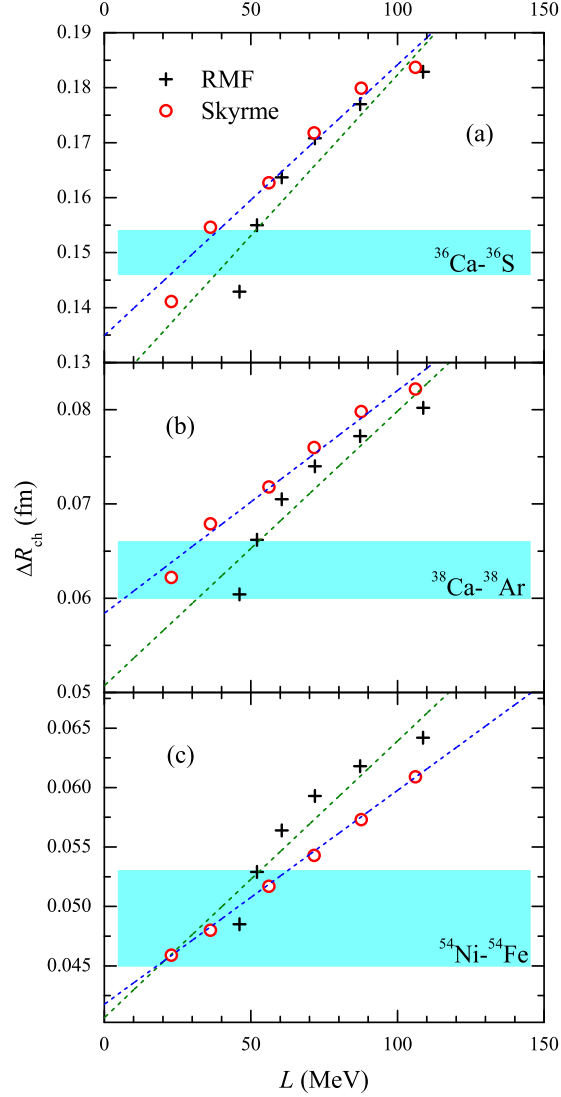


FIG. 1. (Color online) ΔR_{ch} of the mirror partner nuclei ^{36}Ca - ^{36}S (a), ^{38}Ca - ^{38}Ar (b) and ^{54}Ni - ^{54}Fe (c) as a function of slope parameter L at saturation density ρ_0 . The experimental result is shown as a horizontal light blue band. The crosses are results of relativistic EDFs and the open circles are for the Skyrme EDFs calculations. The dashed lines indicate theoretical linear fits.

In order to make further constraints on the EoS of asymmetric nuclear matter, the relations between the symmetry energy at saturation density and the ΔR_{ch} of mirror pairs nuclei can also be evaluated as well as the relation between L and ΔR_{ch} . Therefore, the “Data-to-data” relations between the symmetry energies and these slope parameters are shown in Fig. 3 by various colored planes for $A = 36$ (Ca-S), 38 (Ca-Ar) and 54 (Ni-Fe) mirror-partner nuclei. The plane covered by the shadow slash represents the result of theo-

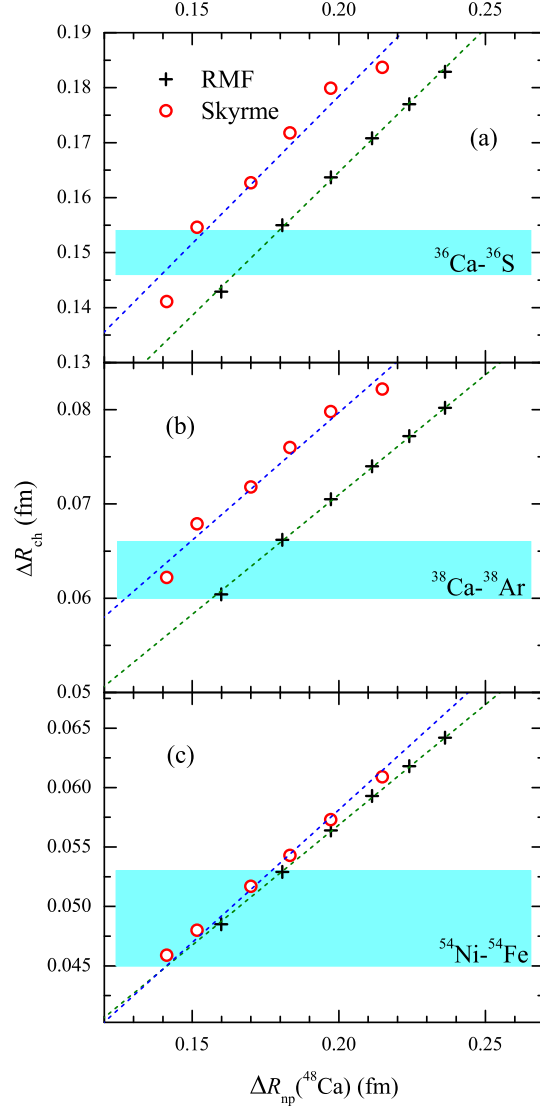


FIG. 2. (Color online) “Data-to-data” relation between ΔR_{ch} of $A = 36, 38$ and 54 mirror-partner nuclei and the neutron skin thickness ΔR_{np} of ^{48}Ca . The same marks and color coding are used as in Fig. 1.

retical prediction. From this figure, it is noticeably found that the deduced symmetry energy locates at the interval of $E_s = 29.89\text{-}31.85$ MeV and the slope of the symmetry energy covers the range of $L = 22.50\text{-}51.55$ MeV.

To facilitate the quantitative comparison of the extracted results with those theoretical calculations, various available estimates of the slope parameter L of symmetry energy are shown in Fig. 4. It is evidently noted that our present result has a remarkable overlap with the results obtained by various methods or observables. Our calculations can predominantly

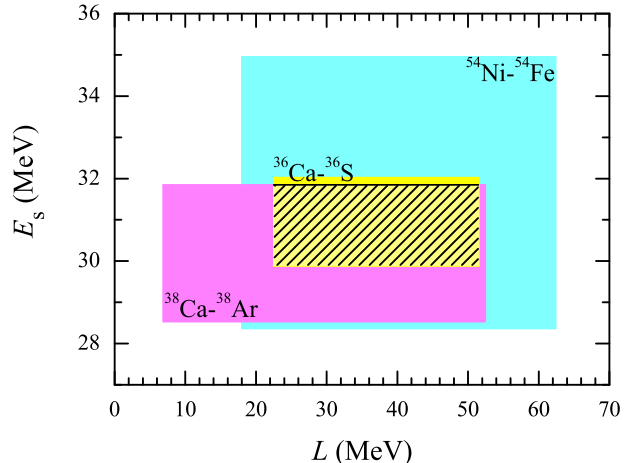


FIG. 3. (Color online) Symmetry energy E_s and the slope of symmetry energy L are limited by the ΔR_{ch} of $A = 36$ (yellow plane), 38 (light purple panel) and 54 (light blue plane) mirror-partner nuclei. The plane covered by the shadow slash represents the result of theoretical prediction in this work.

cover the result for L extracted from the PDR in the ^{132}Sn ($L = 29.0\text{-}82.0$ MeV) but fairly deviate from ^{68}Ni ($L = 50.3\text{-}89.4$ MeV) [25]. In Fig. 4, it shows the weighted average value in the interval of 64.8 ± 15.7 MeV. In addition, the electric dipole polarizability of a heavy nucleus is very sensitive to both the magnitude and the slope parameter of symmetry energy, which gives the value of $L = 47.3 \pm 7.8$ MeV [26]. By exploiting the correlation together with the experimental values for the isoscalar and isovector giant quadrupole resonance (GQR) energies, the slope parameter of symmetry energy is estimated as $L = 37 \pm 18$ MeV [28]. One can find that both theoretical results can essentially cover the current uncertainty in this work.

The neutron skin thickness Δr_{np} in heavy nuclei provides an alternative terrestrial probes to place restrictions on the nuclear symmetry energy. In Ref. [67], the quite accuracy value of $L = 58 \pm 18$ MeV is deduced by analyzing the neutron skin data on Sn isotopes and the observables originated from heavy-ion collisions. Our calibrated result can cover the uncertainty of this value. The latest NST of ^{48}Ca detected by the CREX group yields the slope parameter $L = 0 \sim 50$ MeV [68], this is in accord with this work ($L = 22.50\text{-}51.55$ MeV). Significantly, the NST of ^{208}Pb detected by the PREX-II group yields a larger value of $L = 76 \sim 165$ MeV. Reed et al. [19] have reported a comparable interval of the slope

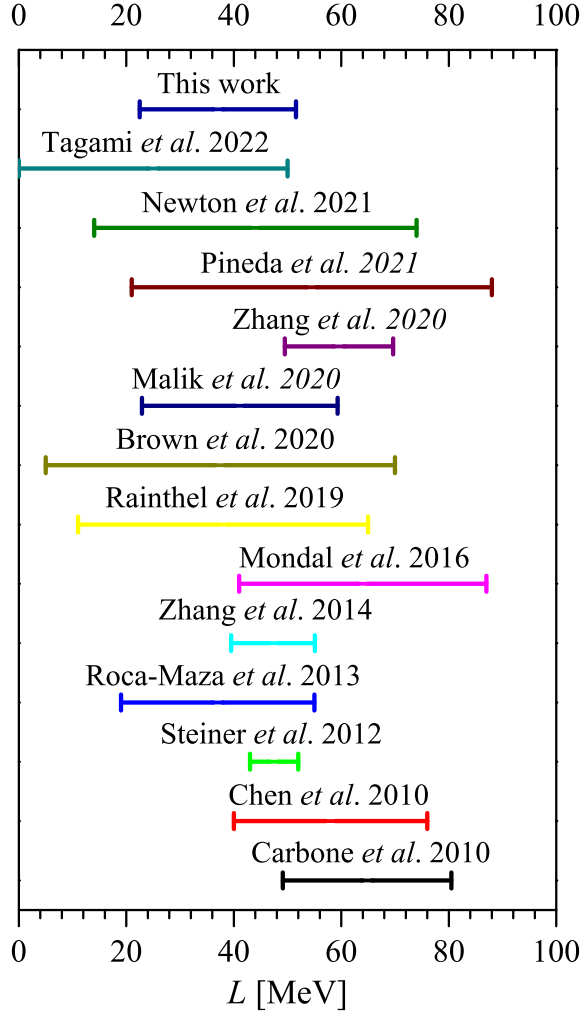


FIG. 4. (Color online) Comparison between the values of L extracted in this work and those from the existing literature. We partly compare the values extracted from various models: Carbone *et al.* [25], Chen *et al.* [67], Steiner *et al.* [71], Roca-Maza *et al.* [28], Zhang *et al.* [26], Mondal *et al.* [13], Raithel *et al.* [50], Brown *et al.* [53], Malik *et al.* [72], Zhang *et al.* [70], Pineda *et al.* [54], Newton *et al.* [76], Tagami, *et al.* [68].

parameter $L = 106 \pm 37$ MeV. These values partially cover the interval range of $L = 54 \sim 97$ MeV induced by heavy-ion collisions [69]. However, the evaluated range in this literature has no overlap with respect to the slope parameter L arising from PREX-II.

In Ref. [70], more information, such as heavy-ion collision data, neutron skin of ^{208}Pb , and tidal deformability and the maximum mass of neutron dense object, has been used to calibrate the values of symmetry energy. This leads to the slope of symmetry energy $L = 59.57 \pm 10.06$ MeV and the quantitative uncertainty is further reduced with respect

to Ref. [67]. Moreover, the slope parameter L can be constrained by various observed astrophysical messages except the terrestrial nuclear experiments. The currently available neutron star mass and radius measurements provide an important constraint on the EoS of neutron matter through quantum Monte Carlo simulations, in which the slope parameter L locates at the range of 43-52 MeV [71]. The correlation of the tidal deformability of a neutron star with the L is studied by sk Λ 267 model, which gives the range of $L = 41.1 \pm 18.2$ MeV [72]. The range of $L = 11-65$ MeV can also be extracted from the observation of the gravitational-wave event of the neutron star merger GW170817 [50]. Our calibrated range ($L = 22.50-51.55$ MeV) is overlapping significantly with these deduced values.

Recently emerging Bayesian framework has been developed widely to study the bulk properties of finite nuclei, e.g., predictions in the nuclear charge radii [73, 74] and nuclear equation of state [75]. The existing database of neutron skin and the bulk properties of nuclear matter are characterized by the prior input quantities, which leads to the credible values of $L = 40^{+34}_{-26}$ MeV and $L = 37^{+9}_{-8}$ MeV [76], respectively. All those evaluated values are consistent with the range of L in this work.

IV. SUMMARY AND OUTLOOK

The microscopic methods based on families of non-relativistic and relativistic EDFs are employed to characterize a systematic variation of isoscalar and isovector properties of the corresponding nuclear matter equations of state. We can conclude that our systematic analysis of the extraction of the slope parameter L from the difference of mirror-partner nuclei charge radii is able to provide a firm result. This may lead us to determine quite accurately the density dependence of symmetry energy that is fundamental quantity for nuclear physics and for their implications in the study of neutron stars.

The linear fits are performed between the differences of charge radii of mirror-partner nuclei and the slope parameter L . As suggested in Refs. [77–81], the precise descriptions of nuclear charge radii are influenced by various mechanisms. Meanwhile, the precise measurement of the charge density distributions usually affects the neutron skin thickness of finite nuclei in quantitative level. In Ref. [82], it demonstrates that the difference of charge radii of mirror pairs nuclei is systematically influenced by the pairing correlations. For weakly bound nuclei, the configuration mixing should be discreetly taken into account in tackling

the pairing correlations [83]. Hence this work should be further reviewed.

V. ACKNOWLEDGEMENTS

This work is partly supported by the Key Laboratory of High Precision Nuclear Spectroscopy, Institute of Modern Physics, Chinese Academy of Sciences. This work is also supported in part by the National Natural Science Foundation of China under Grants No. 12135004, No. 11635003, No. 11961141004. L.-G. C. acknowledges the support of the National Natural Science Foundation of China under Grants No. 12275025, No. 11975096 and the Fundamental Research Funds for the Central Universities (2020NTST06).

-
- [1] A. W. Steiner, M. Prakash, J. M. Lattimer, et al., Isospin asymmetry in nuclei and neutron stars. *Phys. Rept.* 411, 325 (2005). <https://doi.org/10.1016/j.physrep.2005.02.004>
 - [2] B.-A. Li, L.-W. Chen, and C. M. Ko, Recent progress and new challenges in isospin physics with heavy-ion reactions. *Phys. Rept.* 464, 113 (2008). <https://doi.org/10.1016/j.physrep.2008.04.005>
 - [3] F. Ji, J. N. Hu, S. S. Bao, et al., Effects of nuclear symmetry energy and equation of state on neutron star properties. *Phys. Rev. C* 100, 045801 (2019). <https://doi.org/10.1103/PhysRevC.100.045801>
 - [4] Z. Qian, R. Y. Xin and B. Y. Sun, Moments of inertia of neutron stars in relativistic mean field theory: The role of the isovector scalar channel. *Sci. China-Phys. Mech. Astron.* 61, 082011 (2018). <https://doi.org/10.1007/s11433-018-9182-3>
 - [5] J. F. Xu, C. J. Xia, Z. Y. Lu, et al., Symmetry energy of strange quark matter and tidal deformability of strange quark stars. *Nucl. Sci. Tech.* 33, 143 (2022). <https://doi.org/10.1007/s41365-022-01130-x>
 - [6] J. M. Lattimer and M. Prakash, Neutron star observations: Prognosis for equation of state constraints. *Phys. Rept.* 442, 109 (2007). <https://doi.org/10.1016/j.physrep.2007.02.003>
 - [7] M. Baldo and G. Burgio, The nuclear symmetry energy. *Prog. Part. Nucl. Phys.* 91, 203 (2016). <https://doi.org/10.1016/j.ppnp.2016.06.006>

- [8] X. Roca-Maza and N. Paar, Nuclear equation of state from ground and collective excited state properties of nuclei. *Prog. Part. Nucl. Phys.* 101, 96 (2018). <https://doi.org/10.1016/j.pnpnp.2018.04.001>
- [9] M. B. Tsang, J. R. Stone, F. Camera, et al., Constraints on the symmetry energy and neutron skins from experiments and theory. *Phys. Rev. C* 86, 015803 (2012). <https://doi.org/10.1103/PhysRevC.86.015803>
- [10] M. Centelles, X. Roca-Maza, X. viñas, et al., Nuclear symmetry energy probed by neutron skin thickness of nuclei. *Phys. Rev. Lett.* 102, 122502 (2009). <https://doi.org/10.1103/PhysRevLett.102.122502>
- [11] P.-G. Reinhard and W. Nazarewicz, Information content of a new observable: The case of the nuclear neutron skin. *Phys. Rev. C* 81, 051303(R) (2010). <https://doi.org/10.1103/PhysRevC.81.051303>
- [12] Z. Zhang and L.-W. Chen, Constraining the symmetry energy at subsaturation densities using isotope binding energy difference and neutron skin thickness. *Phys. Lett. B* 726, 234 (2013). <https://doi.org/10.1016/j.physletb.2013.08.002>
- [13] C. Mondal, B. K. Agrawal, M. Centelles, et al., Model dependence of the neutron-skin thickness on the symmetry energy. *Phys. Rev. C* 93, 064303 (2016). <https://doi.org/10.1103/PhysRevC.93.064303>
- [14] M. Liu, Z.-X. Li, N. Wang, et al., Exploring nuclear symmetry energy with isospin dependence in neutron skin thickness of nuclei. *Chin. Phys. C* 35, 629 (2011). <https://doi.org/10.1088/1674-1137/35/7/006>
- [15] X.-H. Fan, J.-M. Dong, and W. Zuo, Symmetry energy at subsaturation densities and the neutron skin thickness of ^{208}Pb . *Sci. China-Phys. Mech. Astron.* 58, 062002 (2015). <https://doi.org/10.1007/s11433-015-5673-8>
- [16] C. Xu, Z.-Z. Ren and J. Liu, Attempt to link the neutron skin thickness of ^{208}Pb with the symmetry energy through cluster radioactivity. *Phys. Rev. C* 90, 064310 (2014). <https://doi.org/10.1103/PhysRevC.90.064310>
- [17] J. Xu, W.-J. Xie and B.-A. Li, Bayesian inference of nuclear symmetry energy from measured and imagined neutron skin thickness in $^{116,118,120,122,124,130,132}\text{Sn}$, ^{208}Pb , and ^{48}Ca . *Phys. Rev. C* 102, 044316 (2020). <https://doi.org/10.1103/PhysRevC.102.044316>

- [18] D. Adhikari, H. Albataineh, D. Androic, et al. (PREX Collaboration), Accurate determination of the neutron skin thickness of ^{208}Pb through parity-violation in electron scattering. *Phys. Rev. Lett.* 126, 172502 (2021). <https://doi.org/10.1103/PhysRevLett.126.172502>
- [19] B. T. Reed, F. J. Fattoyev, C. J. Horowitz, et al., Implications of PREX-2 on the equation of state of neutron-rich matter. *Phys. Rev. Lett.* 126, 172503 (2021). <https://doi.org/10.1103/PhysRevLett.126.172503>
- [20] P. Danielewicz, Surface symmetry energy. *Nucl. Phys. A* 727, 233 (2003). <https://doi.org/10.1016/j.nuclphysa.2003.08.001>
- [21] M. Liu, N. Wang, Z.-X. Li, et al., Nuclear symmetry energy at subnormal densities from measured nuclear masses. *Phys. Rev. C* 82, 064306 (2010). <https://doi.org/10.1103/PhysRevC.82.064306>
- [22] B. A. Brown, Constraints on the Skyrme equations of state from properties of doubly magic nuclei. *Phys. Rev. Lett.* 111, 232502 (2013). <https://doi.org/10.1103/PhysRevLett.111.232502>
- [23] N. Wan, C. Xu and Z.-Z. Ren, Density slope of the symmetry energy $L(\rho_0)$ constrained by proton radioactivity. *Phys. Rev. C* 94, 044322 (2016). <https://doi.org/10.1103/PhysRevC.94.044322>
- [24] P. Danielewicz and J. Lee, Symmetry energy II: Isobaric analog states. *Nucl. Phys. A* 922, 1 (2014). <https://doi.org/10.1016/j.nuclphysa.2013.11.005>
- [25] A. Carbone, G. Colò, A. Bracco, et al., Constraints on the symmetry energy and neutron skins from pygmy resonances in ^{68}Ni and ^{132}Sn . *Phys. Rev. C* 81, 041301 (2010). <https://doi.org/10.1103/PhysRevC.81.041301>
- [26] Z. Zhang and L.-W. Chen, Constraining the density slope of nuclear symmetry energy at subsaturation densities using electric dipole polarizability in ^{208}Pb . *Phys. Rev. C* 90, 064317 (2014). <https://doi.org/10.1103/PhysRevC.90.064317>
- [27] L.-G. Cao and Z.-Y. Ma, Symmetry energy and isovector giant dipole resonance in finite nuclei. *Chin. Phys. Lett.* 25, 1625 (2008). <https://doi.org/10.1088/0256-307X/25/5/028>
- [28] X. Roca-Maza, M. Brenna, B. K. Agrawal, et al., Giant quadrupole resonances in ^{208}Pb , the nuclear symmetry energy, and the neutron skin thickness. *Phys. Rev. C* 87, 034301 (2013). <https://doi.org/10.1103/PhysRevC.87.034301>
- [29] L.-G. Cao, X. Roca-Maza, G. Colò, et al., Constraints on the neutron skin and symmetry energy from the anti-analog giant dipole resonance in ^{208}Pb . *Phys. Rev. C* 92, 034308 (2015).

- <https://doi.org/10.1103/PhysRevC.92.034308>
- [30] X. Roca-Maza, L.-G. Cao, G. Colò, et al., Fully self-consistent study of charge-exchange resonances and the impact on the symmetry energy parameters. *Phys. Rev. C* 94, 044313 (2016). <https://doi.org/10.1103/PhysRevC.94.044313>
- [31] A. Krasznahorkay, N. Paar, D. Vretenar, et al., Anti-analog giant dipole resonances and the neutron skin of nuclei. *Phys. Lett. B* 720, 428 (2013). <https://doi.org/10.1016/j.physletb.2013.02.043>
- [32] S.-H. Cheng, J. Wen, L.-G. Cao, et al., Neutron skin thickness of ^{90}Zr and symmetry energy constrained by charge exchange spin-dipole excitations. *Chin. Phys. C* 47, 024102 (2023). <https://doi.org/10.1088/1674-1137/aca38e>
- [33] M. Colonna, V. Baran, and M. Di Toro, Theoretical predictions of experimental observables sensitive to the symmetry energy. *Eur. Phys. J. A* 50, 30 (2014). <https://doi.org/10.1140/epja/i2014-14030-1>
- [34] M. Colonna, Fluctuations and symmetry energy in nuclear fragmentation dynamics. *Phys. Rev. Lett.* 110, 042701 (2013). <https://doi.org/10.1103/PhysRevLett.110.042701>
- [35] G.-F. Wei, X. Huang, Q.-J. Zhi, et al., Effects of the momentum dependence of nuclear symmetry potential on pion observables in Sn + Sn collisions at 270 MeV/nucleon. *Nucl. Sci. Tech.* 33, 163 (2022). <https://doi.org/10.1007/s41365-022-01146-3>
- [36] Y. J. Wang, C. C. Guo, Q. F. Li, et al., The effect of symmetry potential on the balance energy of light particles emitted from mass symmetric heavy-ion collisions with isotopes, isobars and isotones. *Sci. China-Phys. Mech. Astron.* 55, 2407-2413 (2012). <https://doi.org/10.1007/s11433-012-4922-3>
- [37] A. Ono, J. Xu, M. Colonna, et al., Comparison of heavy-ion transport simulations: Collision integral with pions and Δ resonances in a box. *Phys. Rev. C* 100, 044617 (2019). <https://doi.org/10.1103/PhysRevC.100.044617>
- [38] G. Jhang, J. Estee, J. Barney, et al., Symmetry energy investigation with pion production from Sn+Sn systems. *Phys. Lett. B* 813, 136016 (2021). <https://doi.org/10.1016/j.physletb.2020.136016>
- [39] J. Estee, W. G. Lynch, C. Y. Tsang, et al. (S π RIT Collaboration), Probing the symmetry energy with the spectral pion ratio. *Phys. Rev. Lett.* 126, 162701 (2021). <https://doi.org/10.1103/PhysRevLett.126.162701>

- [40] M. B. Tsang, Y. Zhang, P. Danielewicz, et al., Constraints on the density dependence of the symmetry energy. *Phys. Rev. Lett.* 102, 122701 (2009). <https://doi.org/10.1103/PhysRevLett.102.122701>
- [41] Z.-Q. Feng and G.-M. Jin, Probing high-density behavior of symmetry energy from pion emission in heavy-ion collisions. *Phys. Lett. B* 683, 140 (2010). <https://doi.org/10.1016/j.physletb.2009.12.006>
- [42] M. A. Famiano, T. Liu, W. G. Lynch, et al., Neutron and proton transverse emission ratio measurements and the density dependence of the asymmetry term of the nuclear equation of state. *Phys. Rev. Lett.* 97, 052701 (2006). <https://doi.org/10.1103/PhysRevLett.97.052701>
- [43] W.-J. Xie, J. Su, L. Zhu, et al., Symmetry energy and pion production in the Boltzmann-Langevin approach. *Phys. Lett. B* 718, 1510 (2013). <https://doi.org/10.1016/j.physletb.2012.12.021>
- [44] W.-J. Xie and F.-S. Zhang, Nuclear collective flows as a probe to the neutron-proton effective mass splitting. *Phys. Lett. B* 735, 250 (2014). <https://doi.org/10.1016/j.physletb.2014.06.050>
- [45] H. Yu, D.-Q. Fang and Y.-G Ma, Investigation of the symmetry energy of nuclear matter using isospin-dependent quantum molecular dynamics. *Nucl. Sci. Tech.* 31, 61 (2020). <https://doi.org/10.1007/s41365-020-00766-x>
- [46] W. D. Tian, Y.-G Ma, X. Z. Cai, et al., Isospin and symmetry energy study in nuclear EOS. *Sci. China-Phys. Mech. Astron.* 54, 141-148 (2011). <https://doi.org/10.1007/s11433-011-4424-8>
- [47] M. Colonna, Y.-X. Zhang, Y.-J. Wang, et al., Comparison of heavy-ion transport simulations: Mean-field dynamics in a box. *Phys. Rev. C* 104, 024603 (2021). <https://doi.org/10.1103/PhysRevC.104.024603>
- [48] M. C. Miller, F. K. Lamb, A. J. Dittmann, et al., PSR J0030+0451 mass and radius from NICER data and implications for the properties of neutron star matter. *Astrophys. J.* 887, L24 (2019). <https://doi.org/10.3847/2041-8213/ab50c5>
- [49] G. Raaijmakers, S. K. Greif, K. Hebeler, et al., Constraints on the dense matter equation of state and neutron star properties from NICERs massCradius estimate of PSR J0740+6620 and multimessenger observations. *Astrophys. J. Lett.* 918, L29 (2021). <https://doi.org/10.3847/2041-8213/ac089a>

- [50] C. A. Raithel and F. Özel, Measurement of the nuclear symmetry energy parameters from gravitational-wave events. *Astrophys. J.* 885, 121 (2019). <https://doi.org/10.3847/1538-4357/ab48e6>
- [51] N. Wang and T. Lin, Shell and isospin effects in nuclear charge radii. *Phys. Rev. C* 88, 011301(R) (2013). <https://doi.org/10.1103/PhysRevC.88.011301>
- [52] B. A. Brown, Mirror charge radii and the neutron equation of state. *Phys. Rev. Lett.* 119, 122502 (2017). <https://doi.org/10.1103/PhysRevLett.119.122502>
- [53] B. A. Brown, K. Minamisono, J. Piekarewicz, et al., Implications of the $^{36}\text{Ca} - ^{36}\text{S}$ and $^{38}\text{Ca} - ^{38}\text{Ar}$ difference in mirror charge radii on the neutron matter equation of state. *Phys. Rev. Research* 2, 022035 (2020). <https://doi.org/10.1103/PhysRevResearch.2.022035>
- [54] S. V. Pineda, K. König, D. M. Rossi, et al., Charge radius of neutron-deficient ^{54}Ni and symmetry energy constraints using the difference in mirror pair charge radii. *Phys. Rev. Lett.* 127, 182503 (2021). <https://doi.org/10.1103/PhysRevLett.127.182503>
- [55] A. J. Miller, K. Minamisono, A. Klose, et al., Proton superfluidity and charge radii in proton-rich calcium isotopes. *Nature Phys.* 15, 432 (2019). <https://doi.org/10.1038/s41567-019-0416-9>
- [56] J. Xu, Z. Zhang, and B.-A. Li, Bayesian uncertainty quantification for nuclear matter incompressibility. *Phys. Rev. C* 104, 054324 (2021) <https://doi.org/10.1103/PhysRevC.104.054324>
- [57] M. Bender, P.-H. Heenen, and P.-G. Reinhard, Self-consistent mean-field models for nuclear structure. *Rev. Mod. Phys.* 75, 121 (2003). <https://doi.org/10.1103/RevModPhys.75.121>
- [58] D. Vretenar, A. Afanasjev, G. Lalazissis, et al., Relativistic Hartree-Bogoliubov theory: static and dynamic aspects of exotic nuclear structure. *Phys. Rept.* 409, 101 (2005). <https://doi.org/10.1016/j.physrep.2004.10.001>
- [59] H. Liang, J. Meng and S.-G. Zhou, Hidden pseudospin and spin symmetries and their origins in atomic nuclei. *Phys. Rept.* 570, 1 (2015). <https://doi.org/10.1016/j.physrep.2014.12.005>
- [60] G. Colò, (private communication).
- [61] J. Piekarewicz, Pygmy resonances and neutron skins. *Phys. Rev. C* 83, 034319 (2011). <https://doi.org/10.1103/PhysRevC.83.034319>
- [62] G. Colò, N. Van Giai, J. Meyer, et al., Microscopic determination of the nuclear incompressibility within the nonrelativistic framework. *Phys. Rev. C* 70, 024307 (2004). <https://doi.org/10.1103/PhysRevC.70.024307>

- [63] D. Adhikari, H. Albatineh, D. Androic, et al., Electric dipole polarizability of ^{48}Ca and implications for the neutron skin. *Phys. Rev. Lett.* 118, 252501 (2017). <https://doi.org/10.1103/PhysRevLett.118.252501>
- [64] J. Birkhan, M. Miorelli, S. Bacca, et al. (CREX Collaboration), Precision determination of the neutral weak form factor of ^{48}Ca . *Phys. Rev. Lett.* 129, 042501 (2022). <https://doi.org/10.1103/PhysRevLett.129.042501>
- [65] M. K. Gaidarov and I. Moumene and A. N. Antonov, et al., Proton and neutron skins and symmetry energy of mirror nuclei. *Nucl. Phys. A* 1004, 122061 (2020). <https://doi.org/10.1016/j.nuclphysa.2020.122061>
- [66] F. Sammarruca, Proton skins, neutron skins, and proton radii of mirror nuclei. *Front. Phys.* 6, 90 (2018). <https://doi.org/10.3389/fphy.2018.00090>
- [67] L.-W. Chen, C. M. Co, B.-A. Li, et al., Density slope of the nuclear symmetry energy from the neutron skin thickness of heavy nuclei. *Phys. Rev. C* 82, 024321 (2010). <https://doi.org/10.1103/PhysRevC.82.024321>
- [68] S. Tagami, T. Wakasa and M. Yahiro, Slope parameters determined from CREX and PREX2. *Results in Physics* 43, 106037 (2022). <https://doi.org/10.1016/j.rinp.2022.106037>
- [69] Y.-Y. Liu, Y.-J. Wang, Y. Cui, et al., Insights into the pion production mechanism and the symmetry energy at high density. *Phys. Rev. C* 103, 014616 (2021). <https://doi.org/10.1103/PhysRevC.103.014616>
- [70] Y.-X. Zhang, M. Liu, C.-J. Xia, et al., Constraints on the symmetry energy and its associated parameters from nuclei to neutron stars. *Phys. Rev. C* 101, 034303 (2020). <https://doi.org/10.1103/PhysRevC.101.034303>
- [71] A. W. Steiner and S. Gandolfi, Connecting neutron star observations to three-body forces in neutron matter and to the nuclear symmetry energy. *Phys. Rev. Lett.* 108, 081102 (2012). <https://doi.org/10.1103/PhysRevLett.108.081102>
- [72] T. Malik, B. K. Agrawal, C. Providência, et al., Unveiling the correlations of tidal deformability with the nuclear symmetry energy parameters. *Phys. Rev. C* 102, 052801 (2020). <https://doi.org/10.1103/PhysRevC.102.052801>
- [73] X.-X. Dong, R. An, J.-X. Lu, et al., Nuclear charge radii in Bayesian neural networks revisited. *Phys. Lett. B* 838, 137726 (2023). <https://doi.org/10.1016/j.physletb.2023.137726>

- [74] X.-X. Dong, R. An, J.-X. Lu, et al., Novel Bayesian neural network based approach for nuclear charge radii. *Phys. Rev. C* 105, 014308 (2022). <https://doi.org/10.1103/PhysRevC.105.014308>
- [75] W.-J. Xie and B.-A. Li, Bayesian inference of high-density nuclear symmetry energy from radii of canonical neutron stars. *Astrophys. J.* 883, 174 (2019). <https://doi.org/10.3847/1538-4357/ab3f37>
- [76] W. G. Newton and G. Crocombe, Nuclear symmetry energy from neutron skins and pure neutron matter in a Bayesian framework. *Phys. Rev. C* 103, 064323 (2021). <https://doi.org/10.1103/PhysRevC.103.064323>
- [77] R. An, S.-S Zhang, L.-S Geng, et al., Charge radii of potassium isotopes in the RMF (BCS)* approach. *Chin. Phys. C* 46, 054101(2022). <https://doi.org/10.1088/1674-1137/ac4b5c>
- [78] R. An, X. Jiang, L.-G. Cao, et al., Odd-even staggering and shell effects of charge radii for nuclei with even Z from 36 to 38 and from 52 to 62. *Phys. Rev. C* 105, 014325 (2022). <https://doi.org/10.1103/PhysRevC.105.014325>
- [79] P.-G. Reinhard, W. Nazarewicz, and R. F. Garcia Ruiz, Beyond the charge radius: The information content of the fourth radial moment. *Phys. Rev. C* 101, 021301 (2020). <https://doi.org/10.1103/PhysRevC.101.021301>
- [80] P.-G. Reinhard and W. Nazarewicz, Nuclear charge densities in spherical and deformed nuclei: Toward precise calculations of charge radii. *Phys. Rev. C* 103, 054310 (2021). <https://doi.org/10.1103/PhysRevC.103.054310>
- [81] R. An, L.-S. Geng, and S.-S. Zhang, Novel ansatz for charge radii in density functional theories. *Phys. Rev. C* 102, 024307 (2020). <https://doi.org/10.1103/PhysRevC.102.024307>
- [82] P.-G. Reinhard and W. Nazarewicz, Information content of the differences in the charge radii of mirror nuclei. *Phys. Rev. C* 105, L021301 (2022). <https://doi.org/10.1103/PhysRevC.105.L021301>
- [83] R. An, L.-S. Geng, S.-S. Zhang, et al., Particle number conserving BCS approach in the relativistic mean field model and its application to $^{32-74}\text{Ca}$. *Chin. Phys. C* 42, 114101 (2018). <https://doi.org/10.1088/1674-1137/42/11/114101>